Journal of the Oceanographical Society of Japan
Vol. 41, pp. 65 to 72, 1985

Dynamics of Subtidal Flow in the Taiwan Strait*

Wen-Ssn Chuang†

Abstract: Two current meter moorings were deployed in the Taiwan Strait from 3 April to 5 May 1983. The data indicate that the subtidal flow in this rather wide strait can be separated into two parts: the mean flow and wind-driven flow, which make about equal contributions to the overall flow. The mean flow is probably originates from branching of the Kuroshio through Bashi Channel. The magnitude of the current is nearly 30 cm sec^{-1} flowing northward, and the corresponding along-strait sea surface slope is on the order of 10^{-7}. The residual flow is a local wind-driven flow, and reaches a frictionally balanced state in about 4 hr. Assuming a linear drag law for the bottom stress, a hindcast scheme is constructed and the results compare well with the observations.

1. Introduction

Taiwan Strait is located between Taiwan and mainland China and varies from 160 to 200 km in width (Fig. 1). As part of the East China continental shelf, the strait is rather shallow with an average depth of about 55 m. To the north, the strait is connected to the East China Sea which is essentially a broad continental shelf extending hundreds of kilometers offshore. To the south, the strait is open to the South China Sea where the shelf gradually narrows. A submarine trough is also present which connects the strait to the Bashi Channel and the deeper portion of the South China Sea.

Studies of the dynamics of flow in sea straits, first presented by Defant in 1930 (see Defant, 1961), have tended to concentrate on straits that connect open ocean with otherwise enclosed marginal seas (*e.g.*, the Strait of Gibraltar). Defant found that flow in such straits is primarily governed by the characteristics of the water masses produced in the marginal seas. Since then, the emphasis on sea strait research has been oriented toward a fuller understanding of the nature of the exchange. However, little attention has been paid to accessing the role of sea straits in the framework of regional oceanographic processes (Conlon, 1981).

Parallel to the rapid development of estuarine and coastal oceanography during the last two decades, a new dimension has been added to the study of the dynamics of strait flow in additon to the classical picture of thermohaline circulation. For example, Garrett and Toulany (1981) found that the flow through the Strait of Belle Isle was driven by sea level differences between opposite ends of the strait produced by large-scale meteorological forcing. On the other hand, Conlon (1981) found that the flow in Tsugaru Strait, which is also driven by an along-strait pressure gradient, is caused by a northward drop in coastal sea level of the Tsushima current at the entrance to the strait.

Such a broad view of strait flow dynamics is essential when considering the Taiwan Strait.

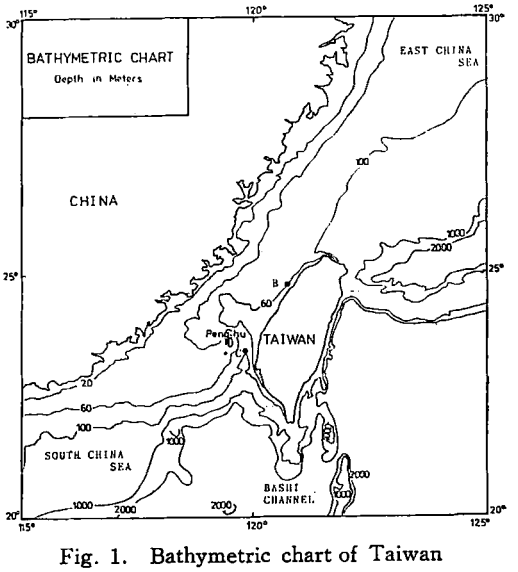

Fig. 1. Bathymetric chart of Taiwan Strait and vicinity.

* Received 8 May 1984; accepted 8 January 1985.
† Institute of Oceanography, National Taiwan University, Taipei, Taiwan, R.O.C.

As much as three different water masses have been identified in this strait (Chu, 1963). They are associated with the China coastal current from the East China Sea, the South China Sea current, and an offshoot of the Kuroshio. The differences in water properties of each current may lead to a baroclinic pressure gradient within the strait. Such a pressure gradient, however, can easily be overpowered by atmospheric forcing due to the broadness and shallowness of the strait. This is demonstrated by the observed seasonal flow reversal accompanying a change in the direction of monsoon winds (mostly from ship reports during 1950's or ealier, see Fig. 2 of Nitani, 1972).

A dynamical interpretation of the low-frequency (nontidal) variability of the strait flow can only be made through continuous direct current measurements. Taking into account the annual variation in the wind field, year-long data are clearly required, which is indeed the objective of an ongoing study (1984-1985) entitled "Experiment in the Strait of Taiwan" (EXIST). Prior to that, a one month pilot study was conducted in 1983, which provides a data base for the present preliminary investigation of the important factors controlling the flow field.

2. Observations

Two current meter moorings were deployed in the pilot study, one was located in the northern part of the strait (Station B, Fig. 1) where the topography is rather flat (actual water depth is 55 m), the other at the head of the trough between Taiwan and Peng-hu Island (Station C) where the depth is about 100 m. A current meter (Aanderaa, RCM-4) was attached to each mooring at 14 m and 20 m above bottom at Stations B and C, respectively. The recorded data cover the period from 3 April to 5 May 1983, when a transition from northeast to southwest monsoon winds was expected.

In studying strait dynamics, one is particularly interested in the alongstrait component of flow. While the choice is rather arbitrary (*e.g.*, the trend of local isobath, the orientation of the nearest coastline, or the axis of the strait), I take the direction of the measured mean flow as the along strait direction at each station. This is due to the fact that throughout the study period, there was a steady current persistantly flowing toward the East China Sea as is evident from the progressive vector diagram using the raw data sets which have a 10-min sampling interval (Fig. 2). The defined direction is thus 51°T for Station B, which is very close to the longshore direction, and 2°T for Station C, which is on line with the axis of the trough (see Table 1).

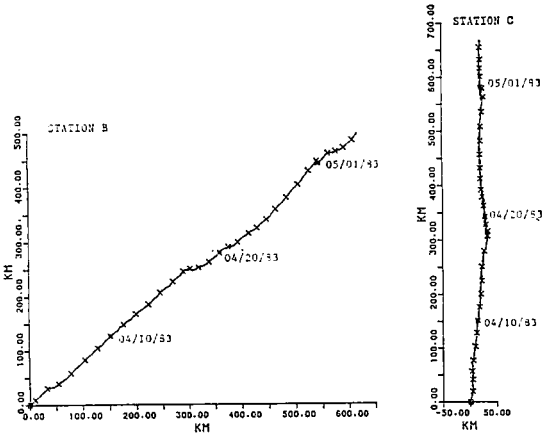

Fig. 2. Progressive diagrams of the measured current (A '+' marks the beginning of each day).

Table 1. Current, windstress and sea level data.

	Unfiltered data								Low-passed data			
	Northward		Eastward		Vector mean			Principale	Along-strait		Cross-strait	
	mean	s.d.	mean	s.d.	mag.	r.m.s.	dir[a]	axis[a]	mean	s.d.	mean	s.d.
Wind stress (0.1 dyne cm^{-2})	−0.5	3.4	−0.6	1.3	0.7	3.7	129°	**18°**	−0.7	3.3	−0.4	0.4
Current (cm sec^{-1})												
Station B	18.0	11.7	22.2	9.8	28.6	32.4	**51°**	38°	28.5	9.6	0.1	4.4
Station C	24.2	52.8	0.8	13.6	24.2	59.6	**2°**	12°	23.8	7.0	−0.1	2.5
Sea level (cm)		67.4								4.3		

[a] Direction and axis angle are measured clockwise from the north, the bold-faceed values are chosen as the along-strait direction.

In order to study the subtidal variations of the flow, the alongshore current component was low-pass filtered to remove the tidal, inertia and other high frequency oscillations using a 5-day Lanczos-cosine filter with a halfpower point set at a period of 40 hr. Also, in an effort to make the best use of these rather short data sets, the low-passed series were extended by 2 days at each end of the record using a 25-hr running mean filter.

Wind and sea level data were obtained at Peng-hu Island (Fig. 1), while windstress was calculated using a constant drag coefficient of 1.4×10^{-3}. The average windstress during the study period is toward the southhwest (Table 1), but the principle axis (18°T) along which the maximum windstress variance occurs lies in a NNE-SSE direction (Kundu and Allen, 1976). Since NNE is indeed the axis of monsoon wind, it is used to obtain the along-strait component of windstress. The 3-hourly raw data was first low-pass filtered with a Lanczos-cosine filter, and then linearly interpolated into an hourly sampled series for later analysis. Hourly sea level data were first adjusted for barometric effect (1 mb$\sim$ 1 cm), then filtered in the same way as the windstress.

3. Analysis and results

Table 1 shows some basic statistics on windstress, currents and sea level. Winds are generally weak and variable during this time of the year. The southwestward mean windstress of 0.07 dyne cm^{-2} corresponds to a wind speed of only 4 knots. Since the variance (square of standard deviation) does not change significantly between the unfiltered and filtered data set, most of the fluctuations occur in the synoptic band. The southwest monsoon wind is not fully established until the end of July when a more steady (larger mean, smaller variance) wind is expected.

The mean current at Stations B and C is strongly affected by local geographic conditions, it flows northward at Station C, and northeastward at Station B. The magnitude is about 20% larger at Station B where the water is shallower. Historical data (Chu, 1963) and some limited hydrographic data obtained while placing the moorings, indicate that the water column is nearly unstratified during this early spring season. The measured currents 14 m or 20 m above the bottom are away from the boundary layer and may well represent the barotropic part of the flow field. As the mean along-strait current and wind are opposite in direction to each other, they do not appear to be directly related. The observed persistent, up-strait drift at velocities of 25 cm sec^{-1}, and accompanying large volume transport to the East China Sea must be induced by some forcing mechanism other than the wind.

Table 2. Current amplitude (in cm sec^{-1}) of the four dominant tidal components.

	M_2	S_2	O_1	K_1
Station B				
Northward	6.9	4.2	2.3	3.8
Eastward	7.1	4.1	3.7	3.0
Station C				
Northward	68.5	24.7	2.9	4.5
Eastward	13.9	5.9	−0.3	0.5

Although the mean flow is smaller at Station C, the variance is larger (almost double), compared with Station B for the unfiltered data. This mainly results from differences in tidal motion at these two stations. From tidal analysis (Foreman, 1978), as shown in Table 2, the tidal current is mostly semi-diurnal at Station C, but a mixture of diurnal and semi-diurnal current occur at Station B. Moreover, the magnitude of the M_2 tide, which is the dominant component at both stations, is about an order of magnitude larger at Station B than Station C (70 cm sec^{-1} compared with 10 cm sec^{-1}). This spatial variation of tidal motion within the strait is due to the known fact the flood tide comes into the strait from opposite ends and meets midway (at about 24°20′N, or south of Station B). As Station C is located in the narrow and relatively shallow part of a trough, the flooding tidal current is strong, however it turns to an ebb tide before reaching Station B. After the tidal motions are eliminated from the data, the variance at these two stations is found to be comparable. The variance of sea level, measured in the southern part of the strait, has the same features as those of the current at Station C.

Figure 3 shows a general picture of the low-frequency variability in the strait flow. Apart from a mean northward flow, the along-strait components of windstress, current and sea level are all strikingly similar, with sea level being out of phase. In other words, a northward wind

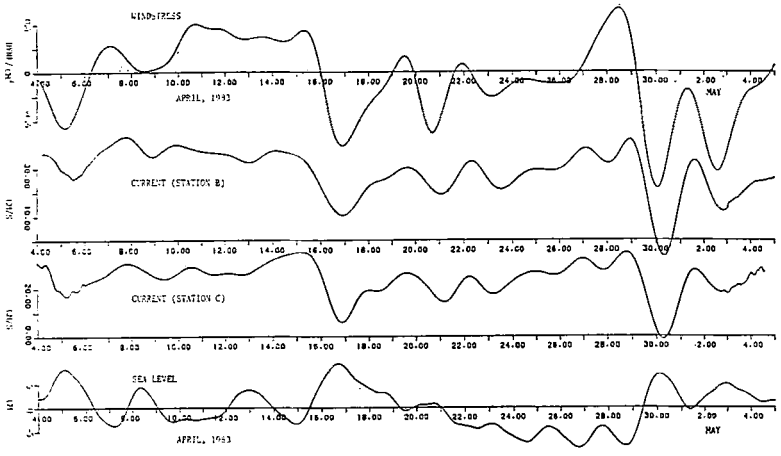

Fig. 3. Time series of the filtered along-strait components of windstress, current, and sea level.

will drive the strait water flowing in the same direction (superimposed on the mean flow) and cause a sea level drop on the west side of the measured current. This phenomenon is the same as that found over many continental shelves where local wind forcing is important (*e.g.*, Smith, 1974; Beardsley and Butman, 1974), and can be satisfactorily explained by the coastal Ekman model with the windstress and bottom stress balanced in the along-strait direction, and the sea surface slope and Coriolis term balanced in the cross-strait direction (Csanady, 1976).

More detailed study of the dynamics of low-frequency variability can best be done using cross-spectrum analysis, however due to the limited time duration (~30 days) and number of events that occurred, the uncertainty in the analysis would be unacceptably high for each of the frequency bands resolved. Instead, linear correlation and regression methods were used to investigate the relationship between pairs of data sets over the entire study period.

The frictional balance between the fluctuating wind and current suggested in Fig. 3 can thus be tested with appropriately parameterized bottom stress. While both quadratic and linear laws have been suggested in the literature, the later was chosen in computing the bottom stress as the background (including tidal) currents are comparable or larger than the wind-induced current components (Winant and Beardsley, 1979). The correlation was indeed significant, γ^2 is 0.66 for Station B and 0.64 for Station C (the 95% significance level is 0.39 and 0.36 for

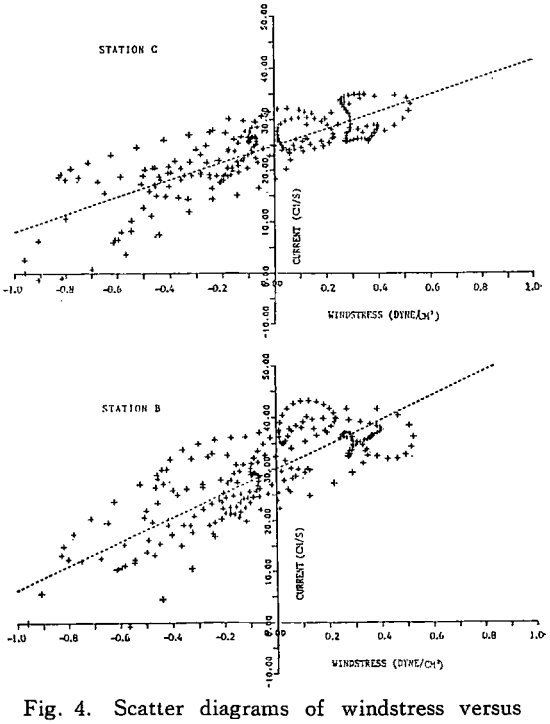

Fig. 4. Scatter diagrams of windstress versus current velocity (at 3-hr sampling interval), with the fitted line resulting from linear regression analysis plotted.

B and C, respectively). On the other hand, the correlation between current and sea level is poor, only 0.28 for Station B and 0.33 for Station C.

Using windstress as the independent variable, regression analysis indicates that the relationship between windstress and current can be fitted to

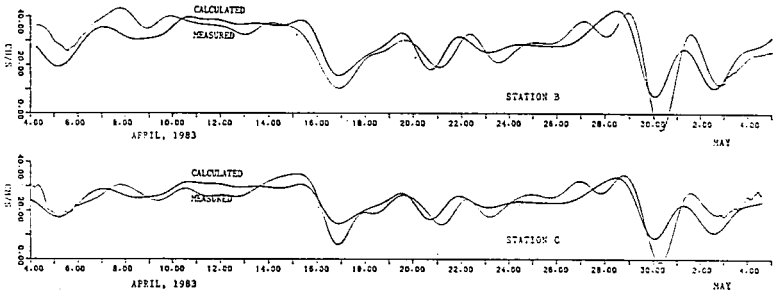

Fig. 5. Measured current and calculated current using zero-lagged windstress data.

a straight line (Fig. 4) with a slope of 24.0 cm sec^{-1} per dyne cm^{-2} and an intercept of 30.1 cm sec^{-1} for Station B, while the corresponding figures for Station C are 17.0 and 24.9, respectively. In other words, a northward 30 cm sec^{-1} current exists at Station B in the absence of wind, and it increases another 24 cm sec^{-1} for a windstress of 1 dyne cm^{-2}. The magnitude of mean flow decreases about 20 % and the ratio drops about 30 % at Station C compared with Station B.

Assuming steady flow in a straight channel, the balance of along-channel momentum for the entire water column is:

$$\tau - \rho r V = \rho g h \frac{\partial \zeta}{\partial y} \qquad (1)$$

where τ, V, and ζ are the windstress, current, and sea level, respectively, and r is a resistance coefficient with the dimension of velocity. The right-hand side of Eq. (1) represents the effective along-strait subsurface pressure gradient which is assumed to be responsible for the observed mean flow. Using the results from regression analysis, the estimated value of r and $\partial\zeta/\partial y$ is 4.17×10^{-2} cm sec^{-2} and -2.33×10^{-7} for Station B (h=55 m), and 5.90×10^{-2} cm sec^{-1} and -1.50×10^{-7} for Station C (h=100 m).

Given the observed wind history, we are thus be able to re-construct a time series of current velocity based on the above analysis. Both the calculated and measured current are depicted in Fig. 5. In general, the hindcast flow is smoother (*i.e.*, lacking some high frequency fluctuations), and weaker at the peak of events. Also, it leads the measured flow by a few hours, especially during the second half of the record. A further analysis was made to determine the time needed for water movement to respond to the wind by computing the lagged correlation between current and windstress. The results indicate that the highest correlation occurred when the wind leads the current by 4 to 5 hr (Fig. 6). This time, which is sometimes referred to as "frictional adjustment time" (Csanady, 1974; Sandstrom, 1980), is required for the water to reach a certain speed that bottom stress balances the imposing windstress. In other words, during this period of time, the energy input from the wind is working to accelerate the fluid. This process is completely neglected in the steady-state model described by Eq. (1).

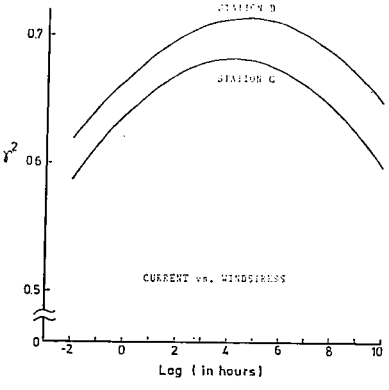

Fig. 6. Correlation between current and lagged windstress.

In order to improve the hindcast, the regression analysis was applied to the data pair of current and 4-hr lagged windstress. The calculated intercept and slope do not show any significant change (less than 3 %) from that of zero-lagged data, however, the predicted currents are more in line with the observations, although underestimation at low speed is still quite obvious (Fig. 7).

4. Discussion

During early spring, the subtidal flow in the

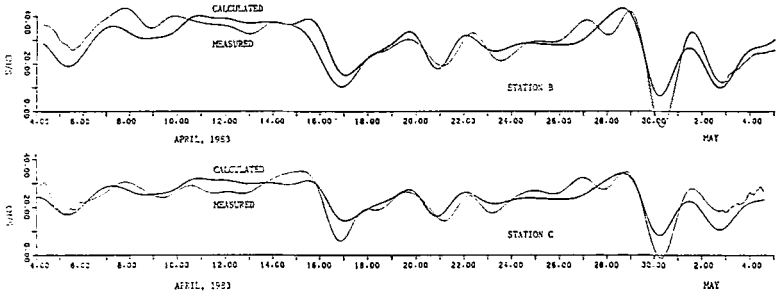

Fig. 7. Measured current and calculated current using 4-hr lagged windstress data.

Taiwan Strait can be conveniently separated into two parts: the mean flow and wind-driven flow, which make about equal contributions to the overall flow. The source of the northward mean flow may be either the South China Sea or the Kuroshio. General circulation in the South China Sea follows the monsoon wind pattern quite closely, and may flow northward only in summer when the southwest monsoon is fully established. The density difference between the East (cold) and South (warm) China Sea water, though probably not small during this time of the year, cannot account for the observed 25 to 30 cm sec^{-1} mean current and the thermohaline circulation should be in the southward direction. Therefore, this mean flow more likely originates as a branch from the Kuroshio that flows into Bashi Channel while the main stream turns northward at the shelf break east of Taiwan (Nitani, 1972).

Without broader coverage, it is difficult to access the amount of Kuroshio water leaving the main stream. It is also not known how much of this branching water flows cyclonically along the depth contour and flows into the South China Sea. Hydrographic data indicate that there is a front present along the 200-m isobath during winter when the northeast monsoon is dominant (Chern, 1982). However, even if only a small amount of the branching Kuroshio water is able to flow northward can still cause a significant current within the strait due to its shallowness, as demonstrated by the observed half knot mean flow.

The incoming Kuroshio water will inevitably raise the level of the sea surface at the southern end of the strait relative to the other end, and hence, develop a pressure gradient sloping northward. In a steady-state situation, it can only be balanced by a bottom stress, or an along-strait flow directed down the gradient, as observed. Using the frictional coefficient calculated from the wind-driven component, the pressure gradient is estimated to be about 2.0×10^{-7}. In other words, a sea surface elevation change of 2 cm in 100 km exists in the strait, which is of the same order of magnitude as in the Mid-Atlantic Bight where intensive study on the sea level slope has been made (Wang, 1979). The slope is not constant in space (it is larger at Station B), which is understandable as the total transport is continuous but the magnitude of flow and corresponding sea surface slope must vary with local geographical conditions.

In regard to fluctuating part of the flow, the observations clearly point to a frictional balance between surface and bottom stress. Although bottom friction has a quadratic relationship to velocity, the averaged form (over a period long compared with tidal cycles) is approximately linearly related to velocity provided that the averaged value is small compared with the instantaneous measurements (Csanady, 1976). The resistance coefficient depends on many factors, *e.g.*, the strength (r.m.s.) of the background current, the depth of water, and the type of sediment on the sea floor. The greater value found at Station C (about 40 % larger) is probably due to the stronger tidal current (Table 2) at that site. In general, the value of 4 to 6×10^{-2} cm sec^{-1} in the strait is about the same as found in many other shelf areas (Winant and Beardsley, 1979), although higher values, on the order of 10^{-1} (Scott and Csanady, 1976; Chuang and Wiseman, 1983), have also been reported.

The time lag between wind and current is about 4 hr. This is quite reasonable as this time lag lies between the short time lag observed in

shallow water (Scott and Csanaby, 1976) and the 9-hr lag observed over a deeper, ordinary shelf (Chao and Pietrafesa, 1980). Therefore, accelerations in the strait are not completely negligible. The other term omitted in the along-strait frictional equilibrium model is the Coriolis force because the integrated onshore flow cannot be large in a channel. The Coriolis force due to along-strait flow, however, becomes very important and must be balanced by a pressure gradient force in the cross-strait direction. The sea level data on one side indeed suggest a relation between sea level and the flow, but the relation is not statistically significant. This is of course understandable as the sea level data from one side of the strait only, cannot represent the sea level slope in the strait. The geostrophic balance can only be checked with a complementary tide gauge deployed in Taiwan, across the strait from Peng-hu. Unfortunately, local sand barriers prohibit such deployment.

Although by including the mean pressure gradient, linearly parameterized bottom friction, and adjustment time, a hindcast scheme for the along-strait current can be constructed based on the observed wind, it is only valid for this particular period when the wind is weak and variable. In other seasons, large scale circulation in the nearby bodies of water must be taken into consideration, and the local wind forcing mechanism may no longer dominate inside the strait. More specifically, the northward penetration of the offshoot from the Kuroshio may not be constant, also the residual circulation may be related to meteorological forcing in some more indirect way, or to some other indices of ocean variability. Thus, flow through the strait is probably best studied through a combination of dynamical models of the response of the nearby regional seas to wind forcing, together with further analysis of yearlong current and sea level measurements in the strait.

Acknowledgements

This study was sponsored by the National Science Council of R.O.C. under grants NSC72-0407-M002a-07 and NSC73-0407-M002a-08.

References

Beardsley, R.C. and B. Butman (1974): Circulation on the New England continental shelf: Response to strong winter storms. Geophys. Res. Lett., **1**, 181-184.

Chao, S.-Y. and L.J. Pietrafesa (1980): The subtidal response of sea level to atmospheric forcing in the Corolina capes. J. Phys. Oceanogr., **10**, 1246-1255.

Chern, C.-S. (1982): A preliminary study on the response of Taiwan Strait to winter monsoon. Acta Oceanogr. Taiwanica, **13**, 124-139.

Chu, T.-Y. (1963): The oceanography of the surrounding waters of Taiwan. Reports of the Institute of Fishery Biology of Ministry of Economic Affairs and National Taiwan University, **1**, 29-44 (in Chinese).

Chuang, W.-S. and W.J. Wiseman (1983): Coastal sea level response to frontal passages on the Louisiana-Texas shelf. J. Geophys. Res., **88**, 2615-2620.

Conlon, D.M. (1981): Dynamics of flow in the region of the Tsugaru Strait. Technical Report No. 312, Coastal Studies Inst., Louisiana State Univ.

Csanady, G.T. (1974): Barotropic currents over the continental shelf. J. Phys. Oceanogr., **4**, 357-371.

Csanady, G.T. (1976): Mean circulation in shallow seas. J. Geophys. Res., **81**, 5389-5399.

Defant, A. (1961): Physical oceanography. Vol. 2, Pergamon Press, New York, 598 pp.

Foreman, M.G.G. (1978): Manual for tidal currents analysis and prediction. Report 78-6, Inst. of Ocean Sci., Particia Bay, Sidney, B.C.

Garrett, C. and B. Toulany (1981): Variability of the flow through the strait of Belle Isle. J. Mar. Res., **39**, 163-189.

Kundu, P.K. and J.S. Allen (1976): Some three-dimensional characteristics of low-frequency current fluctuations near the Oregon coast. J. Phys. Oceanogr., **6**, 181-199.

Nitani, H. (1972): Beginning of Kuroshio. In: Kuroshio, Its Physical Aspects, ed. by H. Stommel and K. Yoshida, Univ. Tokyo Press, Tokyo, pp. 129-163.

Sandstrom, H. (1980): On the wind-induced sea level changes on the Scotian shelf. J. Geophys. Res., **79**, 435-443.

Scott, J.T. and G.T. Csanady (1976): Nearshore currents off Long Island. J. Geophys. Res., **81**, 5401-5409.

Smith, R.L. (1974): A description of current, wind and sea level variations during coastal upwelling off the Oregon coast, July-August 1972. J. Geophys. Res., **85**, 461-468.

Wang, D.-P. (1979): Low frequency sea level variability on the Middle Atlantic Bight. J. Mar. Res., **37**, 683-697.

Winant, C.D. and R.C. Beardsley (1979): A comparison of some shallow wind-driven currents. J. Phys. Oceanogr., **9**, 218-220.

台湾海峡の長周期変動流の力学

荘　　文　思*

要旨：1983年4月3日から5月5日まで台湾海峡の2点に流速計を係留した．測流結果によると，台湾海峡の潮汐周期より長い周期帯の流れは，平均流と吹送流で構成され，それぞれがほぼ等しい大きさであることがわかった．平均流はバシー海峡を経由してきた黒潮の分岐流であると思われる．流速は約 30 cm sec^{-1} の北流であり，海峡を横断して 10^{-3} のオーダーの海面傾斜が生じている．残りの部分は局地的な風による吹送流で，約4時間で海底摩擦とつりあうようになる．流速に比例する摩擦係数を用いて評価した流速値は観測値とほぼ一致した．

* 国立台湾大学海洋研究所
台北市，台湾